Stony Brook University

Structure characterization of adsorbed poly (ethylene oxide) layers on solid substrate

A Thesis Presented

by

Fen Chen

to

The Graduate School

In Partial Fulfillment of the

Requirements

For the Degree of

Master of Science

in

Materials Science and Engineering

Stony Brook University

May 2012

Stony Brook University

The Graduate School

Fen Chen

We, the thesis committee for the above candidate for the

Master of Science degree, hereby recommend

acceptance of this thesis.

Tadanori Koga – Thesis Advisor
Assistant Professor, Materials Science and Engineering

Michael Dudley – Committee Member
Professor, Materials Science and Engineering

T.A.Venkatesh – Committee Member
Assistant Professor, Materials Science and Engineering

This thesis is accepted by the Graduate School

Charles Taber
Interim Dean of the Graduate School

Abstract of the Thesis

Structure characterization of adsorbed poly (ethylene oxide) layers on solid substrate

by

Fen Chen

Master of Science

in

Materials Science and Engineering

Stony Brook University

2012

In recent years, irreversibly adsorbed polymer layers formed on solid substrates have been received considerable interest since they can modify various properties of polymeric materials confined at the nanometer scale. In this thesis, I investigate the annealing time dependence of the poly (ethylene oxide) (PEO) adsorbed layer formed at the substrate interface. The detailed structures of the PEO adsorbed layer prepared were characterized by ellipsometry, atomic force microscopy (AFM), and x-ray reflectivity techniques. The total thickness of the PEO adsorbed layer is generally around 3 nm. Different from PS, the annealing time dependence of the PEO adsorbed layer simple show minor increase when annealing 2hr, then stay the same. $ScCO_2$ and toluene rinse cycle can further reduce the thickness of PS adsorbed layer. For PEO, only toluene rinse is enough to obtain the final adsorbed layer. We discuss the model of the structure of the adsorbed layer, and estimate that there is no crystal structure formed in the PEO adsorbed layer.

Table of Contents

List of Figures

Acknowledgments

First I would like to sincerely thank my academic advisor Prof. Tadanori Koga, for his excellent guidance and constant support during these years. This thesis cannot be finished without his instructions.

The support of my senior Naisheng Jiang and Peter Gin is greatly appreciated. Both of them guided me at every step when I need their advice. They are always available with their suggestions on conducting experiments and useful discussions. They really helped me a lot for my research.

Many thanks to all the group members in Koga research group who provided support by being good friends and providing many valuable suggestions.

Special thanks to all my friends at Stony Brook University and people from Materials Science and Engineering department.

Finally I would like to thank my family for providing love and encouragement to work hard towards my goals.

Chapter 1. Introduction

1.1. Spin cast polymer thin films

Spin coating is widely used for thin film preparation over large areas with high structural uniformity. Emslie *et al.*[1] were firstly to propose a simple model of the spin coating process predicting the flow pattern and the thickness of the resulting films. Later, by other researches[2, 3] showed improved models which are in better agreement with experimental results. Some spin-cast studies have been directed to structures at the molecular level. Cohen and Reich[4] found that high molecular weight polymers exhibited long-range order, up to 10 μm from the substrate, whereas films composed of low M_w polymers were only ordered over a few μm . Many efforts have been made to predict the influence of conditions of film preparation on the properties such as density, expansion/contraction, and stability, providing a general concept that allows designing and adjusting all properties of polymers thin films. Figure 1-1 is the schematic view of a spin-coating process. After complete evaporation of a solvent, a uniform polymer thin film is formed.

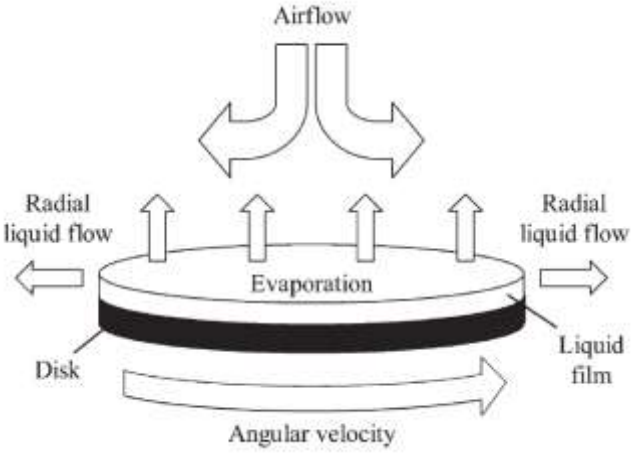

Figure 0-1 Scheme of the spin coat process [4]

Bornside *et al.* [5]divided a spin-coating process into four stages, i.e. deposition, spin-up, spin-off, and solvent evaporation. During the first three stages, film thickness is dictated by the centrifugal forces, but during the final stage, the increasing viscosity of the solution, the rate of the solvent evaporation, and shear thinning of the fluid must be taken into consideration.

1.2. Solvent content in thin spin-coat polymer films

For as spun polymer films, the morphology of the polymer chains is frozen and solvent is still retained due to the very quick evaporation process. [6, 7] The solvent content influences the roughness, charge carrier transport, adhesion strength of adhesive, and the glass transition temperature (T_g). García-Turiel and Jérôme [8] calculated the absolute amount of solvent retention in thin spin-cast films by using gas chromatography(GC). They showed the time dependence of the amount in the films (the thickness ranging from 15-500 nm) after a drying time of 6h. They concluded that the proportion of toluene increases significantly in thinner films (Figure 1-2) and the solvent desorption rate exhibits no variation on the film thickness. Moreover, an enrichment of toluene was found at the Si/polymer interface [8].

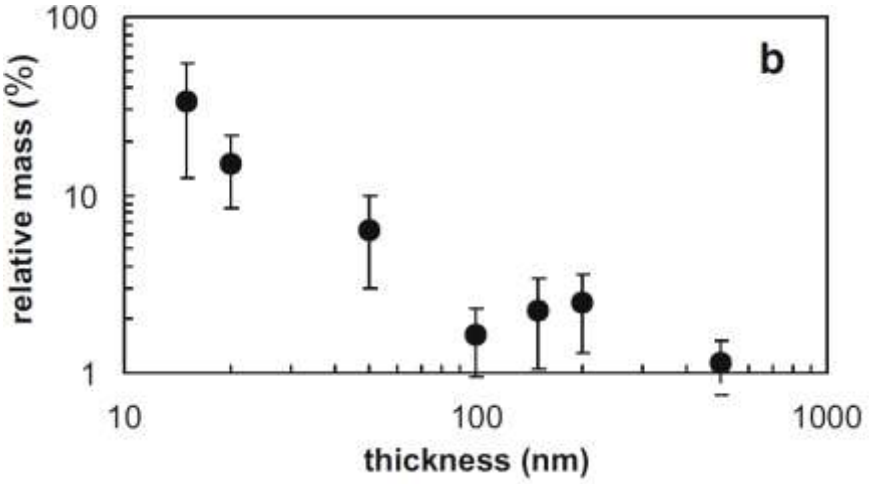

Figure 0-2 Relative amount of toluene retained versus film thickness. [8]

Perlich *et al.* [9] investigated the solvent content in thin deuterated polystyrene (d-PS) films, onto silicon substrates by using neutron reflectometry (NR). Figure 1-3 NR profiles of the films annealed at temperatures below and above T_g. Fig1-3b shows the long-term behavior (over 2 years) of the total retained solvent content φ as a function of time (t). They concluded that under the different annealing and storage conditions tested, the remaining solvent was not totally removed.

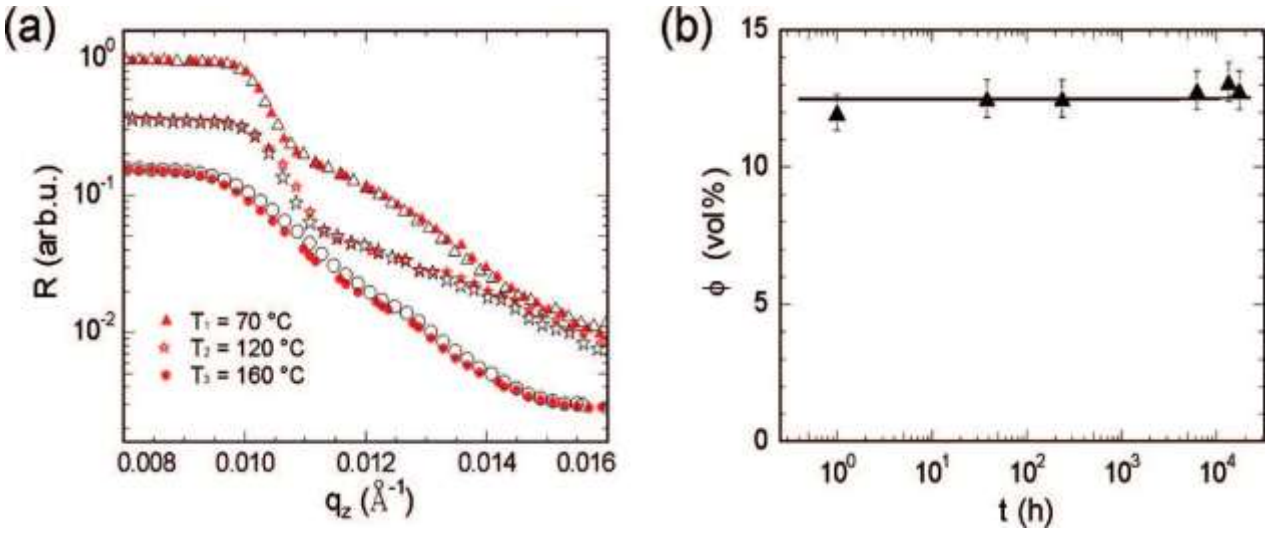

Figure 0-3 (a) High-resolution NR data in the region of total external reflection of thin films as prepared (open symbols) and after annealing (closed symbols) for 8 h at 70 (△, ▲), 120 (☆, ★), and 160 °C (○, ●). For clarity, the curves are shifted along the reflectivity axis. (b) Long-term behavior of the total retained solvent content φ as a function of the time, t, since preparation. The solid line is a guide to the eye. [8]

Spin-cast films represent highly metastable forms of matter [10]. Reiter found that PS films, which are thinner than the coil size, could show an more than 10% increase in thickness when annealed at temperatures ranging from the ambient temperature T_a to the nominal glass transition temperature (T_g). Orts *et al*. [11] studied the temperature dependence of the thicknesses of spin cast PS films prepared on Si substrates by using in situ x-ray reflectivity under vacuum. The PS film shows the contraction ranging from 0%-17% when heated up to 70℃. In the temperature interval from 20 to 70 ℃, the plot of thickness verse T is reversible (Figure 1-4). When the temperature increased above 70℃, the film expands irreversibly by~ 20%, and ultimately dewets (Figure 1-5).

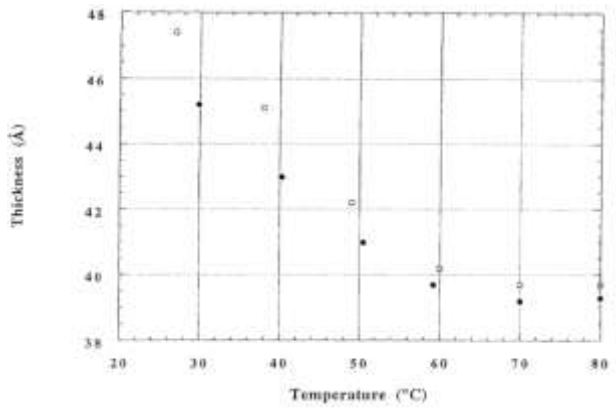

Figure 0-4 Reproducibility of the observed contraction phenomen, An ulrathin PS film was annealed and then subsequently heated incrementally to 80℃ cooled, and reheated to 80℃. (●) the first heating cycle and (○) the second heating cycle. [11]

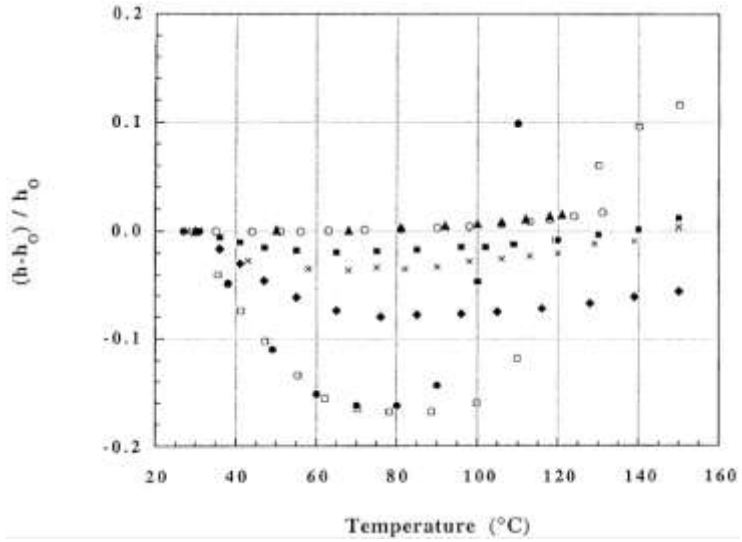

Figure 0-5 Relative change in thickness of PS (Mw=573000) films on Si as a function of temperature. h_o is the initial thickness. h_o are denoted as (●)47.4Å ,(□)49.9Å,(◆)100.4Å, (X) 155.1Å,(■)216.6Å,(○)264.3Å,(▲)833Å [11]

Furthermore, residual stresses in spin cast polymer thin films were found to decrease with increasing annealing time [12], but do not completely vanish even after long annealing above $T_{g,bulk}$. These findings show that non-equilibrated states in ultrathin films are metastable with extremely long-life time. Reiter and Napolitano [13] pointed out that equilibration times could be extraordinarily long if polymer mobility is reduced due to adsorption of the polymer onto the substrate. Consequently, experiments unavoidably have to deal with non-equilibrated polymer thin films.

1.1. Confinement effect of polymer thin films

The confinement of polymers into thin films influences a number of their bulk physical properties including glass transition temperature [14-17], coefficient of thermal expansion, dissolution rate, and diffusion behavior. Frank *et al*. [4] suggested that crystallization doesn't occur below 150 Å in thickness and this critical thickness may represent a critical nucleus thickness for surface-induced crystallization. For the substrate-supported thin films, T_g has been observed to either increase or decrease with decreasing film thickness [18, 19] , depending on the interactions between the polymer and the substrate. A deviation of dynamic properties from the bulk behavior, showing an increase of the relaxation rate was observed starting from the film thickness which is about 3 times larger than the gyration radius of polymer chains [20].

1.2. Polymer crystallization in thin films

The use of ultrathin films to study one-dimensional confinement can examine the confinement effects on crystallization. Frank *et al*. [21] found that the degree of crystallinity decreased with decreasing film thickness , vanishing below about 15 nm, and the crystallization occurs faster for thicker films. Dalnoki-Veress [21] observed a remarkable slowing down of the crystal growth at all temperatures studied for PEO films with a thickness of less than~100 nm, suggesting reductions of the mobility of chains at the crystal/amorphous interface.

Sommer and Reiter [22] presented a simulation model for crystallization of quasi-2D monolayer of PEO adsorbed onto bare silicon wafer, as shown in Figure 1-6.

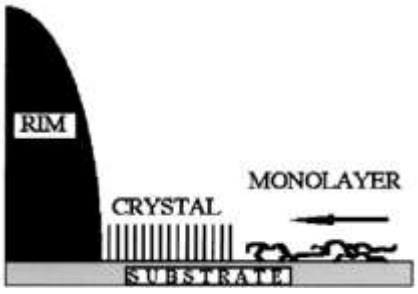

Figure 0-6 Model for crystallization of polymer mono-layer. [21]

The quasi-2D crystals grew by attaching molecules which diffused toward the edge of the crystal. If the probability for desorption from the crystal is low, then the molecules will attach to points at the crystal front, where they arrive first. This is analogous to diffusion limited aggregation,

leading to an instability of the crystal front and eventually, to the formation of fingerlike or fractal patterns.

1.3. Irreversibly adsorbed layer (dead layer) onto the solid substrate

Adsorption of linear polymer chains at the substrate interface is of both practical and theoretical interest and has been the subject of many recent studies. Many of the previous studies have focused on either reversibly adsorbed layer [23, 24] or grafted layers [25]. However, little is known about irreversible adsorption of the polymers [26]. Fujii *et al.* [14] examined if the buried substrate interface of PS/Si films can be oxideized by annealing the films at 150 ℃ in air. Their result shows that a residual film does form on the top of the Si surface, but it is a bound layer of PS. The chain segments attached directly to the substrate are believed to have restricted freedom of movement compared to that are at a distance from the substrate and relatively free. The annealing time dependence of the thickness of the residual film is plotted in Figure 1-7. The residual film continues to grow until about 50h before it saturates. Moreover, their experiments illustrated that the residue films are "soft" and yet stable againt dewetting and rinsing by a good solvent.

The thickness of the surface mobile layer and/or the immobile dead layer near substrate is expected to be at most 10 nm [27].

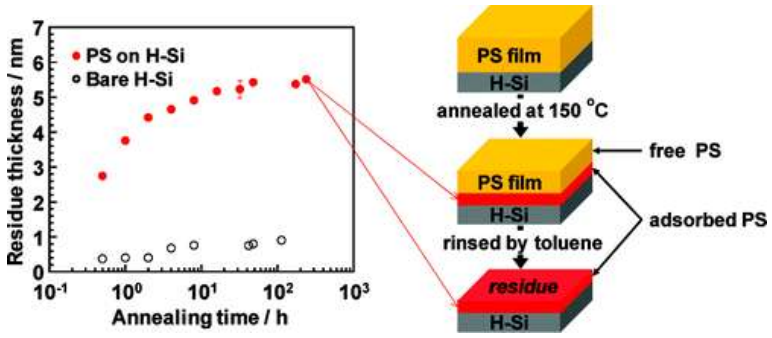

Figure 0-7 Annealing time dependence of the thickness of the residual film obtained from PS/H-Si (solid symbols) and bare H-Si (open symbols).[14]

1.4. Supercritical carbon dioxide ($scCO_2$)

Supercritical CO_2 is becoming an important commercial and industrial solvent due to its role in chemical extraction in addition to its low toxicity and environmental impact. When we consider the application of supercritical CO_2 for polymer processes, it is very important to understand its

interaction with polymers. Although the solubility of polymers in CO_2 is typically very low, the solubility of CO_2 in many polymers is substantial. The important properties such as diffusivity, viscosity, glass transition, melting point, compressibility and expansion can be influenced by the sorption. Especially our research group have found the thermal anomalous swelling of polymer thin films due to the density fluctuations in the fluid phase [28]. The swollen structures can be then preserved by using vitrification of polymer via rapid quench.

The scheme of $scCO_2$ process is schematically shown in Figure 1-8. The swelling of the polymer can lead to dramatic reduction of T_g, i.e., the plasticization effect, even at modest pressures. The plasticization effect is largely determined by polymer-solvent interactions and solvent size. Under pressurized condition, CO_2 molecules can easily permeate into polymers, especially amorphous polymers.

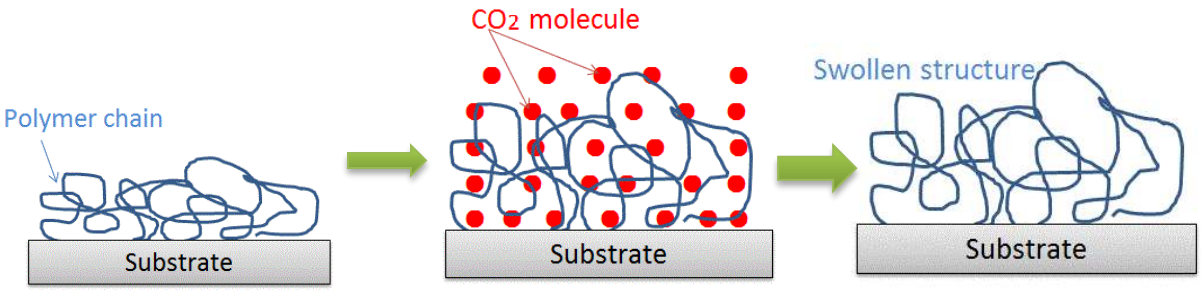

Figure 0-8 Schematic concept of the $scCO_2$ –based processing polymer thin films.

$ScCO_2$ has been employed to manipulate and control surface properties of polymer thin films. Yong Yang *et al*. [29] observed that polymer chains can diffuse discernibly in the surface region even below the bulk T_g. The presence of CO_2, even at low pressures, both expedited the diffusion process and increased the mobile surface layer. Furthermore, Lan *et al*. [30] showed that chain mobility of the polymer was strongly increased in $scCO_2$ when the film thickness was decreased to the scale of radius of gyration of the polymer.

1.5. Density fluctuating $scCO_2$ for polymer thin films

Supercritical phase occurs at a temperature and pressure above its critical point, where it shows both gas-like diffusivity and gas like dissolvability, as seen in Figure 1-9 [28, 31]. Moreover, in the supercritical regime, minor changes in pressure or temperature can result in great changes in the density.

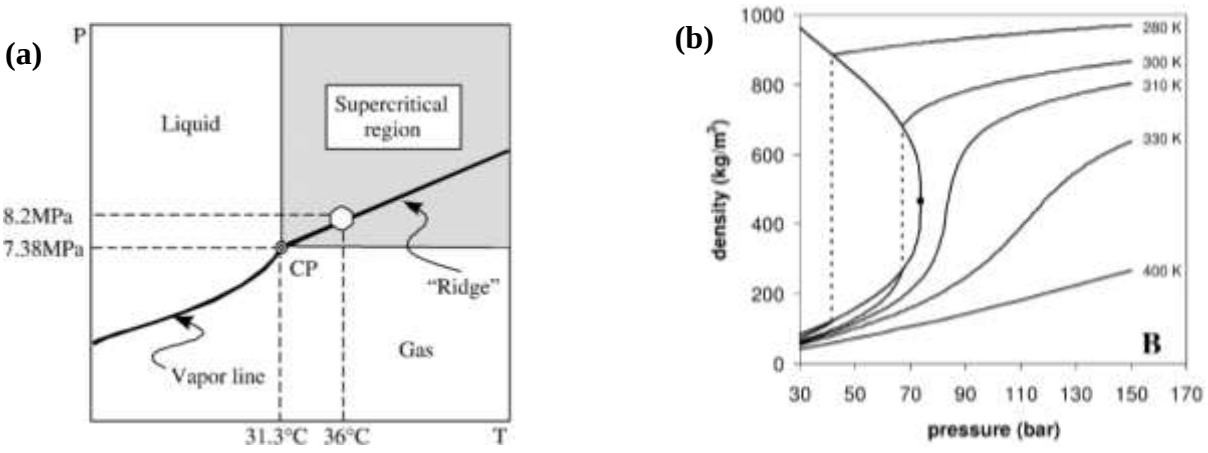

Figure 0-9 (a) Phase diagram of CO_2 near critical point and density fluctuation ridge for CO_2 (b). Density of CO_2 as a function of pressure at different temperatures (solid lines) and at the vapor-liquid equilibrium line (dashed line) [28, 31]

According to the molecular dynamics simulations of a two-dimensional Lennard-Jones fluid, $scCO_2$ is composed of inhomogeneous regions with high and low density, resulting in density fluctuation. Density fluctuations,$< (\Delta N)^2 > / < N >$, can be expressed by using κ_T:

$$< (\Delta \mathbf{N})^2 > / < \mathbf{N} > = (\mathbf{N}/\mathbf{V})\boldsymbol{\kappa}_\mathbf{T}\boldsymbol{\kappa}_\mathbf{B}\mathbf{T} \qquad \textbf{(eq.1)}$$

where N is the number of molecules in the corresponding volume V, κ_B is the Boltzman constant, κ_T is the isothermal compressibility, and T is the thermodynamic absolute temperature [28]. Huang *et al*. [32] shows that the locus of the peaks in the curves forms a "ridge" of the density fluctuations, where it separates the more liquid-like and more gas-like regimes in the supercritical region, as seen in Figure 1-9 (a). Along the ridge, the maximum or minimum of various physical quantities of SCFs, such as isothermal compressibility, thermal conductivity and partial molar volumes, is observed. Wang *et al*. [33] described a theoretical investigation of critical adsorption of CO_2 on an attractive wall. By calculating the Gibbs adsorption and adsorption layer thickness of the supercritical fluids, they summarized that in all cases (different substrates, different supercritical fluids) that maximum adsorption occurs when the supercritical fluid is near its compressibility maximum.

1.6. Enhanced mobility and screening effects of $scCO_2$ on polymer thin films

Compared to bulk polymers, in the cases of thin film/CO_2 system, polymers crystalize in a broader range of temperature and pressure, coupled with a greatly reduced low limit of temperature for crystallization. Lan *et al*. [30] proposed a three-layer mobility model of polymer

thin films under ambient pressure and CO_2 environments (Figure 1-10), to explain the enhanced polymer mobility due to the excess CO_2 adsorbed at the thin film surface and polymer/substrate interface.

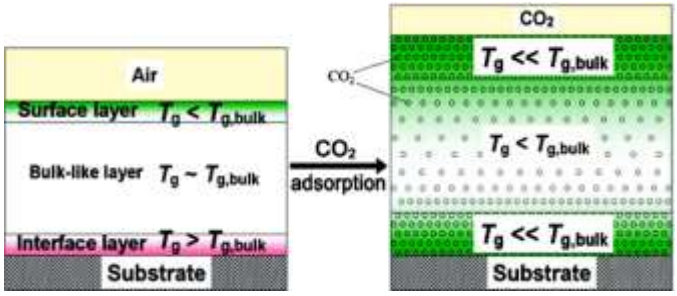

Figure 0-10 schematic illustration of three-layer mobility model, consist of layers with different mobility and T_g [30]

On the other hand, because CO_2 can interact with the hydroxyl groups at the substrate [34], screening the polymer-substrate interactions and hence resulting in enhanced mobility of polymer chains.

1.7. Research motivation

The structure and properties of polymer thin films often deviate significantly from bulk values. Adsorption of linear polymer chains at the substrate interface is of both practical and theoretical interest and has been the subject of many recent studies. However, the majority has been focused on polystyrene (PS), which is an amorphous polymer with its glass transition temperature T_g(100℃). In my thesis, I use poly (ethylene oxide) (PEO), a semi-crystalline polymer with its melting temperature (T_m) of 65℃ to see generality/ differences in adsorbed layers. It should be emphasized that a PEO/SiO_x system exhibits stronger attractive interaction than PS/SiO_x, resulting in different adsorption process.

Chapter 2. Materials and Methods

2.1. Experimental Materials

Polyethylene oxide (PEO, M_w=20,000, Tm=65℃, Aldrich chemistry) was used for the present study. A PEO solution was prepared by dissolving the PEO in toluene (Sigma-Aldrich, ACS reagent, ≥ 99.5%). Different film thicknesses were prepared by the variation of the polymer concentrations in the solutions for spin coating. Solutions were placed on a hot stage for 45 minutes at T= 85℃ in order to thoroughly dissolve the polymer.

2.2. Substrate preparation

The wafers were prepared by rinsing them in distilled water. The first step was performed with a 1:1:1 solution of H_2O: H_2O_2: NH_4OH at 80℃ for 15 minutes in order to remove organic residues. Moreover, this treatment enhances the hydrophilicity of the silicon surface by introducing –OH dangling bonds on them. Inorganic contaminants were rinsed off by applying a 1:1:1 solution of H_2O: H_2O_2: H_2SO_4.The wafers were then thoroughly rinsed with distilled water and then etched by a hydrofluoric acid (HF) solution (HF: H_2O with volume ratio 1:10) in a petri dish to remove a thin oxide layer. The resultant Si wafers an absolutely water free surface.

2.3. Spin coat ultrathin films

PEO thin films were prepared by spin coating at a rotation speed of 2500 rpm for 25s. I prepare a series of PEO thin films with the thickness of 20 nm, 30 nm, 40 nm, 50 nm, 100 nm.

2.4. Anneal the samples

During the spin-coating process, the solvent evaporates rapidly (within a few seconds) and the polymer concentration increases exponentially in time until the film solidifies, resulting in non-equilibrium chain conformations. At this stage, there is a significant amount of solvent remaining in the films. Anneal the samples above $T_{g,bulk}$ for certain time is needed to remove residual stresses induced during spin-coating process.

we annealed films at T=85℃ for various hours, ranging from 0 to 48 hours, then quenched to room temperature rapidly to induce the crystallization.

2.5. Preparation of PEO adsorbed layer

Rinse films in toluene solution on the hot stage at temperature T=60 ℃ every 30mins for about 6~7 times until the thickness stays constant. And then dry the films under vacuum at T=85℃ for 12 hours to remove the residual toluene. According to the studies by Perlich [9] , when annealing temperature is moderately above the T_g, no change or only a minor decrease in remaining solvent content is observed. However, there is a significantly reduction when annealed even higher.

2.6. Ellipsometry

A Rudolph Research Ellipsometer is used to measure the thickness. An ellipsometer relies on the fact that the reflection at a dielectric interface depends on the polarization of the light while the transmission of light through a transparent layer changes the phase of the incoming wave depending on the refractive index of the material. Layers with thickness ranging from 1 nm to several microns can be determined by the ellipsometer. We used a value of 1.455 as the refractive index of PEO.

2.7. Atomic Force Microscopy (AFM)

The surface morphology was characterized by a Digital Nanoscope III AFM in a contact mode to perform topography and friction scans using a Si_3N_4 tip. Images obtained can be analyzed by using Nanoscope programming.

2.8. X-ray reflectivity

X-ray reflectivity is a non-destructive technique used for the structural characterization of multilayers (Figure 2-1). X-ray specular reflectometry can be used to give direct information on layer thickness of thin films and multilayers; surface and interface roughness; surface density gradients and layer density. At the interfaces, a portion x-rays is reflected. Interference of these partially reflected x-ray beams produces a reflectometry pattern. With a high thickness resolution of~0.1 nm, XR presents more precise values compare to other methods like ellipsomoetry.

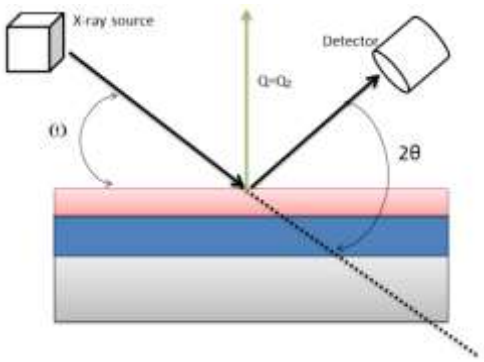

Figure 2-1 X-ray reflectivity measurement geometry

The x-ray reflectivity measurements have been carried out at the x10B beamline of the National Synchrotron Light Source (NSLS), Brookhaven National Laboratory (BNL), using a photon energy 14.2KeV, corresponding to a x-ray wavelength (λ) of 0.87 Å. A Fourier transformation (FT) analysis for XR is useful tool to obtain information related to the interfaces within the multilayers. We use a 3-layer model (i.e. Si, SiO_2, polymer) and 4-layer model (i.e. Si, SiO_2, high density layer, low density layer) to fit the data (Fig 2-2). The x-ray reflectivity experiments are conducted at room temperature.

Figure 2-2 Illustration of 3-layer model (left) and 4-layer model (right) to fit the x-ray reflectivity profile.

2.9. Supercritical carbon dioxide

The supercritical carbon dioxide experiments were conducted at the two density fluctuation conditions where T=36℃ with pressure P=8.2MPa and T=50℃ with pressure P=10.4MPa. The samples were exposed to CO_2 for at least 3h and quickly depressurized to atmospheric pressure within 20 sec.

Chapter 3. Experiment result and discussion

3.1. Thickness dependence of the adsorbed layer

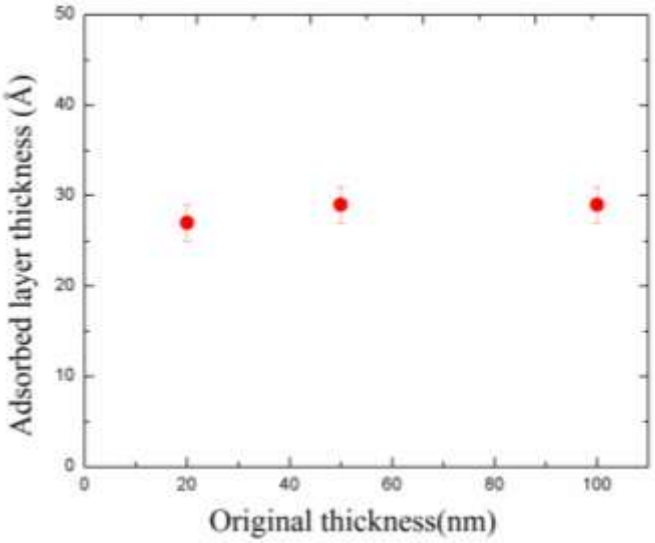

Figure 3-1 Plot of PEO adsorbed layer thickness as a function of initial spin-cast film thickness.

The thickness data obtained from ellipsometer is plotted in Figure 3-1.The results show that the PEO adsorbed layers are in thickness about 3 nm onto the Si substrates regardless of the original thickness. We have known that there exists an adsorbed PS layer on Si substrates.

This phenomenon can be explained by overlapping concentration, c*. The molecular weight dependence on the radius of gyration has been experimentally found to be[35]

$$\mathbf{R_g = 0.215 M_w^{0.583 \pm 0.031}} \qquad \textbf{(eq. 2)}$$

where, M_w denotes the molecular weight of the polymer. In the present study, R_g of PEO is estimated to be 50 Å. Since the individual polymer coils are contiguous to each other at the overlap concentration c^* for the polymer, the radius of gyration can be related to the overlap concentration using the following equation [36]

$$\mathbf{c^* = \frac{3M_w}{4N_A \pi R_g^3}} \qquad \textbf{(eq. 3)}$$

where, N_A is the Avogadro's number. Using eq. (2), c*(PEO) is calculated to be 6.348×10^{-2} g/ml with the density of the toluene($\rho_{Toluene} = 0.8669\ g/ml$), c* by weight percent corresponds to

equals to 7.32%. All the weight concentrations of the solutions used in this study are all lower than c*. Hence, the adsorption process from a dilute concentration is identical.

A representative AFM height image of the adsorbed layer is shown in Figure 3-2. It is clear that no crystal structures are found in the adsorbed layer.

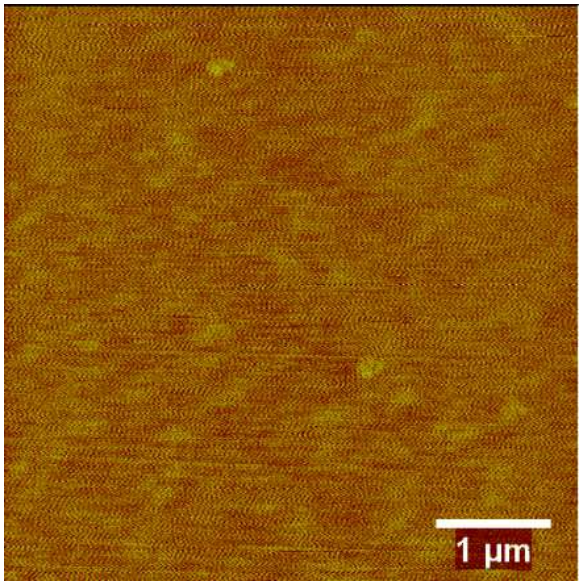

Figure 3-2 AFM height image of PEO adsorbed layer prepared from the 20 nm thick film

3.2. Annealing time dependence of the adsorbed layer thickness

3.2.1. X-ray reflectivity (XR)

Spin-cast 50 nm PEO thin films were annealed under vacuum at 85℃ for different time (0, 1, 2, 3, 5, 12, 24, 48 hours), then rapidly quenched to room temperature, and finally followed by toluene rinse in order to remove the loosely attached chains. Before XR experiments, the samples were dried under vacuum at 85℃ for 12 h to remove the residual solvent in the films.

Figure 3-3 is a representative x-ray reflectivity data for the PEO adsorbed layer. From the FT profile, there are two peaks correspond to the two interfaces, indicating there are two layers in the adsorbed layer. Hence, we use a 4-layer model to fit the x-ray reflectivity data (i.e. Si, SiO_2, bottom layer, top layer).

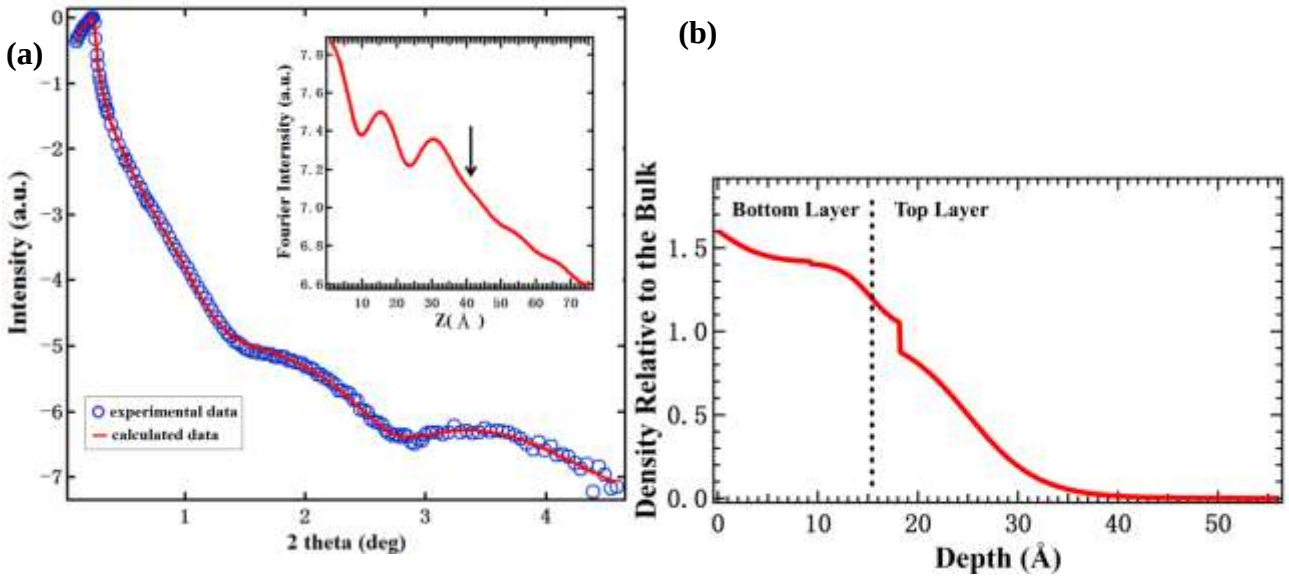

Figure 3-3 (a) Representative x-ray reflectivity profile for the PEO adsorbed layer is shown as symbols with best fittings as lines for the films. FT profile is interted . (b) Adsorbed layer density relative to the bulk.

As shown in Figure 3-4, the observed x-ray reflectivity profile of the adsorbed layer could be fitted by using a 4-layer model for different annealing times. Figure-3-5 summarizes the adsorbed layer thickness as a function of the annealing time.

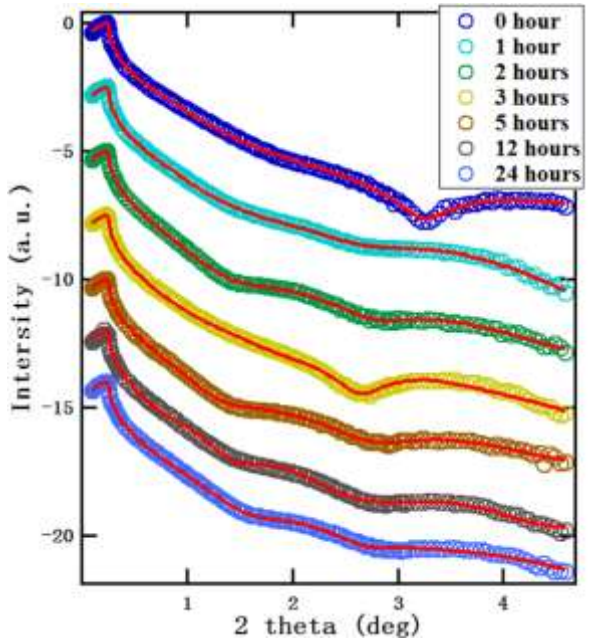

Figure 3-4 X-ray reflectivity data for the adsorbed layer is shown as symbols with fittings as lines for the films that are annealed at 85℃ for differment time.

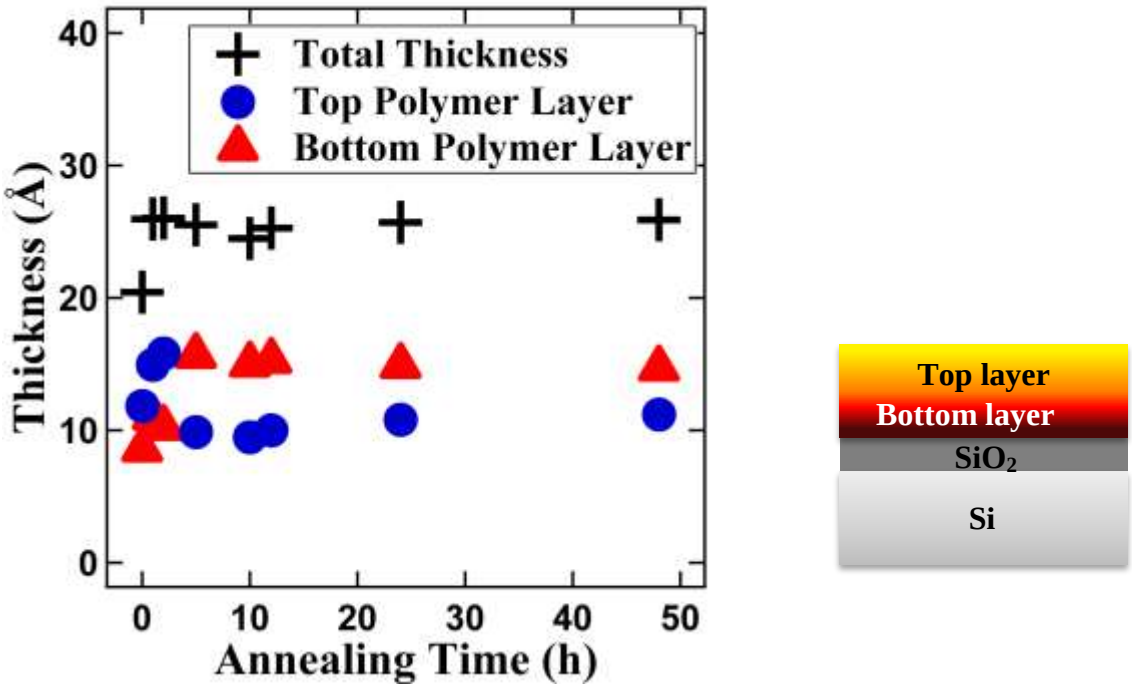

Figure 3-5 Plot of the thickness of the adsorbed layer as a function of annealing time.

From Figure 3-5, the adsorbed layer is formed instantly after the spin-cast process. When the sample was annealed for 2 hours after spin casting, the total thickness of the adsorbed layer increases slightly from 20.4 Å to 26 Å, then the thickness remains almost constant. We also found that the thicknesses of the top and bottom layers are 15.8 Å and 10.2 Å respectively. The bottom layer shows a similar growth curve to the total film thickness.

The dispersion of the adsorbed layer, which is proportional to the densiyt , as a function of annealing time is plotted in Figure 3-6.

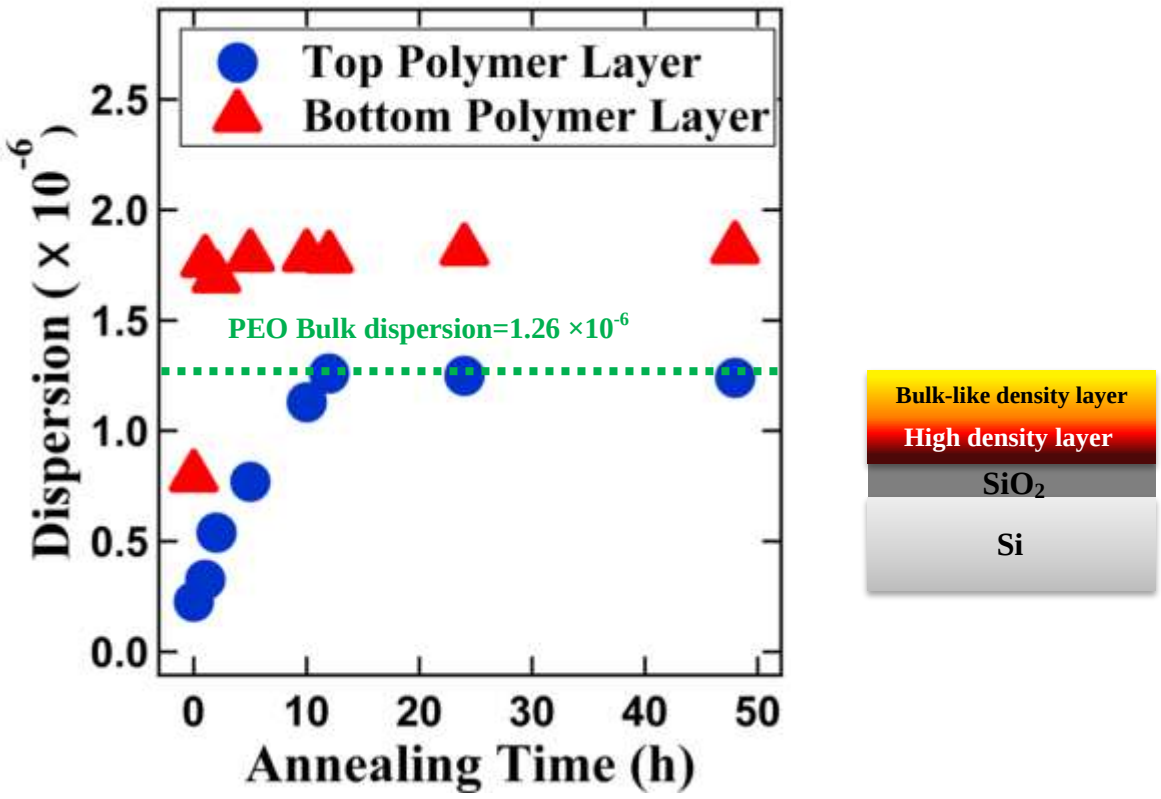

Figure 3-6 Plot of the density of the adsorbed layer as a function of annealing time

From figure 3-6, it can be observed that the dispersion of the bottom layer increases with the annealing time and then becomes constant.($\delta = 1.76 \times 10^{-6}$). δ value of the top layer also increases with the annealing time, and saturated to $\delta = 1.25 \times 10^{-6}$, which corresponds to the bulk δ value of PEO. Therefore, we can conclude that the top layer has a bulklike density while the bottom layer has a much higher density. Note that the adsorbed layers start dewetting when annealed over 24 hours.

The model to illustrate the final adsorbed layer structure from irreversible polymer adsorption is shown in Figure 3-7. As mentioned above, the adsorbed layer consists of two layers, i.e. diffuse outer layer (bulk-like density layer) and the flattened layer (high density layer). This irreversible adsorption process can be divided into two stages. First monomer surface bonds form immediately upon contact and adsorption kinetics are diffusion-controlled. The later stage is the formation of the diffuse outer layer.

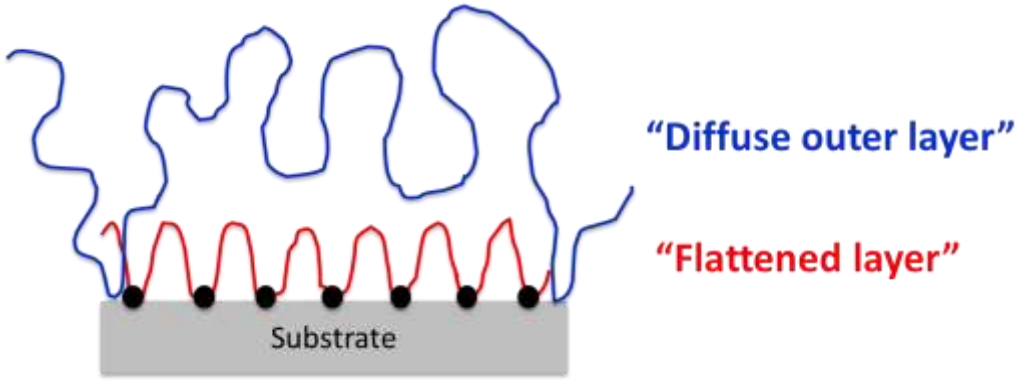

Figure 3-7 Sketch of predicted final layer structure resulting from irreversible polymer adsorption.

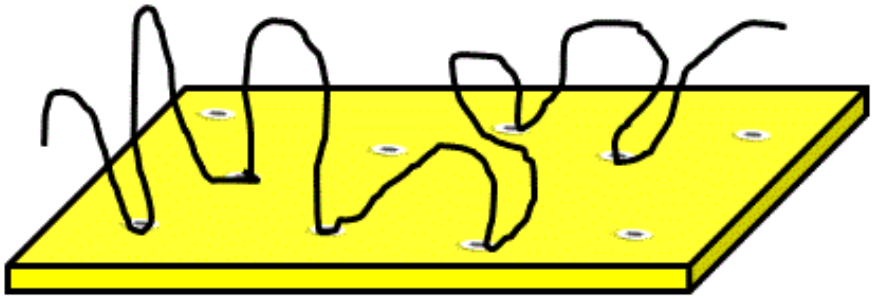

Figure 3-8 Sketch of the configuration of adsorbed chain at late stages of adsorption.

Initially the surface is empty and it is inevitable that any chain whose center of gravity diffuse within the coil size of the surface will adsorb. This attachment of polymer chains is diffusion-controlled and the surface coverage grows. After attachment of the first monomers, the collapse of a single chain into a flattened structure occurs rapidly. The late-coming chains start to see a continuously decreasing density of available sites for adsorption. As the surface approaches saturation, late arrived chains can only be adsorbed at the free empty sites, resulting in a loop between the sites.

There is a question! Can the polymer chain crystalline in the 3 nm adsorbed layer? In order to join the lamella at the growth front, the adsorbed chains have to be desorbed partially to form upright folds conformation. Transition from flatly adsorbed to upright folded states reduces the surface area occupied by a single chain. When crystal growth proceeds, a depletion zone is formed due to more and more unoccupied surface places. Hence, we hypothesize that the polymer chains can't fold within the 3 nm PEO irreversibly adsorbed layer, as indicated by AFM image.

3.2.2. Supercritical CO_2- Toluene cycle

When exposed to $scCO_2$, the polymer chain mobility is increased due to adsorption of CO_2 molecules. Further, previous experiments showed that CO_2 can be used as a screening solvent for polymers and Si substrates. Thus it is possible to further remove the loosely attached chains using CO_2. In fact, our research group showed that for polystyrene adsorbed layer, the unified process of $scCO_2$ and toluene can further remove the loosely attached polymer chains as shown in Figure 3-9. We therefore applied that unified process to PEO adsorbed layer to see whether the adsorbed layer can be further removed.

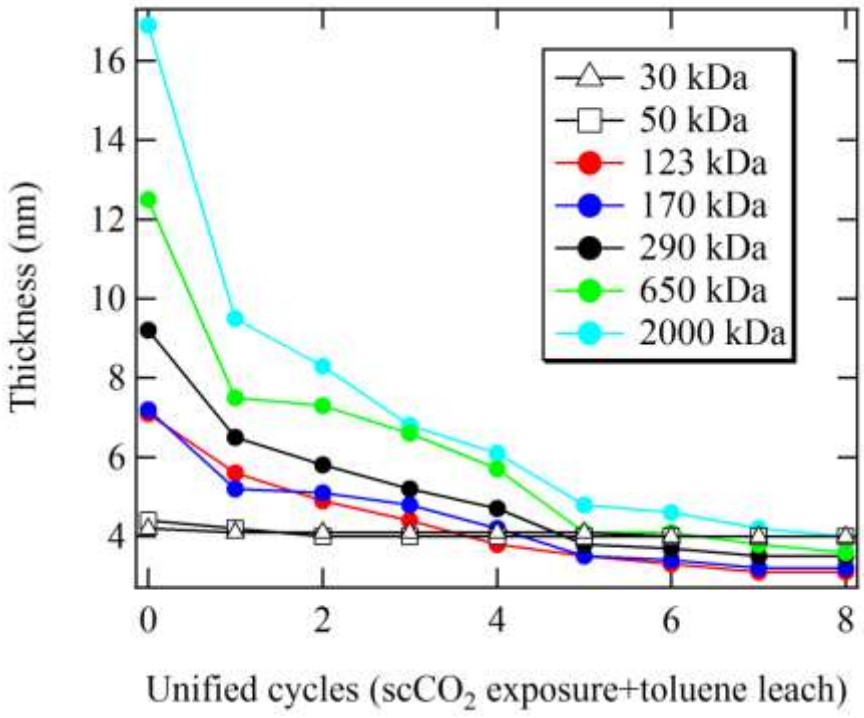

Figure 3-9 Plot of PS adsorbed layer thickness as a function of $scCO_2$ –toluene wash cycles*

*data from Peter Gin

After exposed to supercritical CO_2 at the ridge conditions (36℃, 8.2MPa) and (50℃, 10.4MPa), the films were further rinsed by toluene. After each cycle of the unified leaching process, the thicknesses were measured by ellipsometry, figure 3-10 plots the results. From the figure, we can see that the thickness of the adsorbed layer doesn't change with and without the unified leaching process.

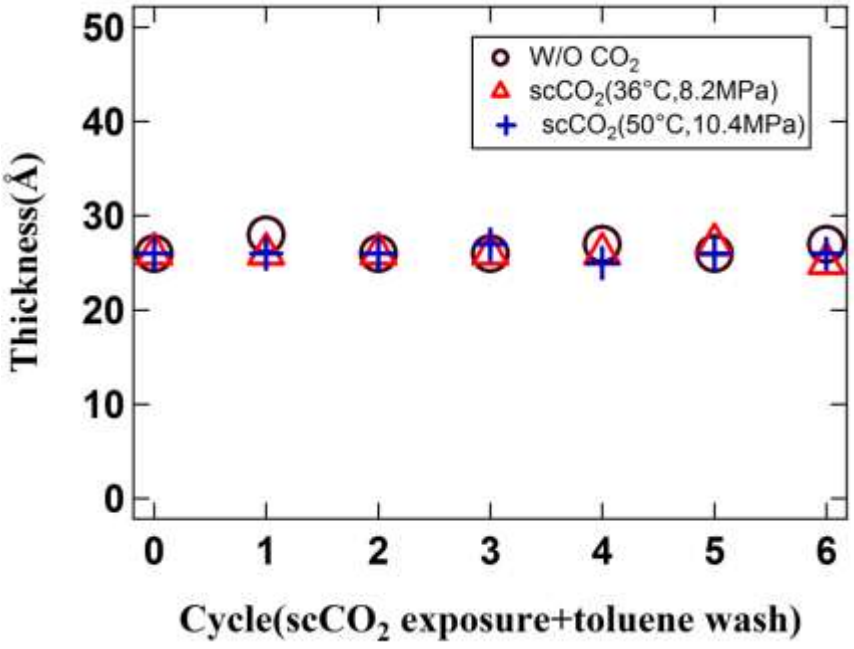

Figure 3-10 Plot of PEO adsorbed layer thickness as a function of $scCO_2$ –toluene wash cycles

Hence, PEO with such a low molecular weight, toluene washing is more than enough to remove the loosely attached polymer chains. This is consistent with the PS adsorbed layer where the thickness of the adsorbed layer remains constant even after the unified leaching process. We hypothesize that with lower molecular weights, it is difficult to form loops between the empty sites.

3.3. Temperature dependence of the adsorbed layer thickness

We also measured the temperature dependence of the adsorbed layer thickness by using x-ray reflectivity. The XR measuremnets were performed under vacuum.

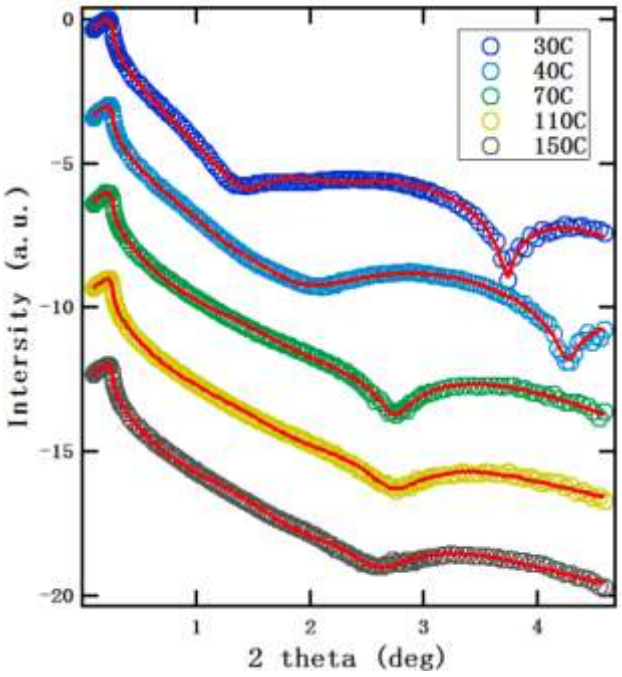

Figure 3-11 X-ray reflectivity data for the adsorbed layer is shown as symbols with fittings as lines for the films measured with elevating temperature

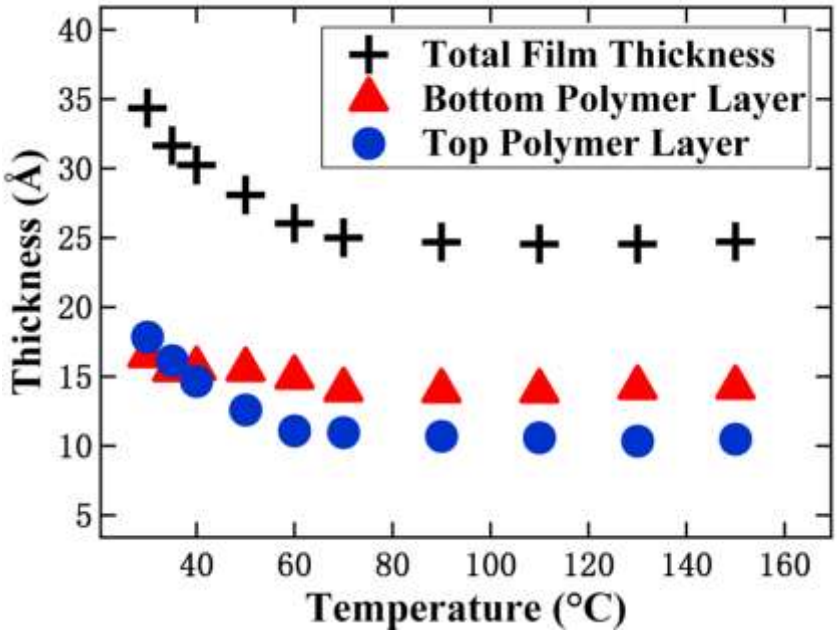

Figure 3-12 The reproducibility of the observed contraction phenomena.

The fim was heated from 30 to 150 ℃ in approximately 10℃ increments and then cooled back to 30 ℃ to see the reproducibility. As shown in Figure 3-12, we can see the contraction and expansion of the PEO adsorbed layer, depending on the T ranges. When the temperature increased to 70℃ , the total thickness of the adsorbed layer first decreases from 35 Å to 25 Å ,and then remains constant above T=70℃. After cooling the film back to room temperature, we found that the thickness returned to 35 Å. Hence, the observed contraction and expansion of the adsorbed film is thermally reversible.

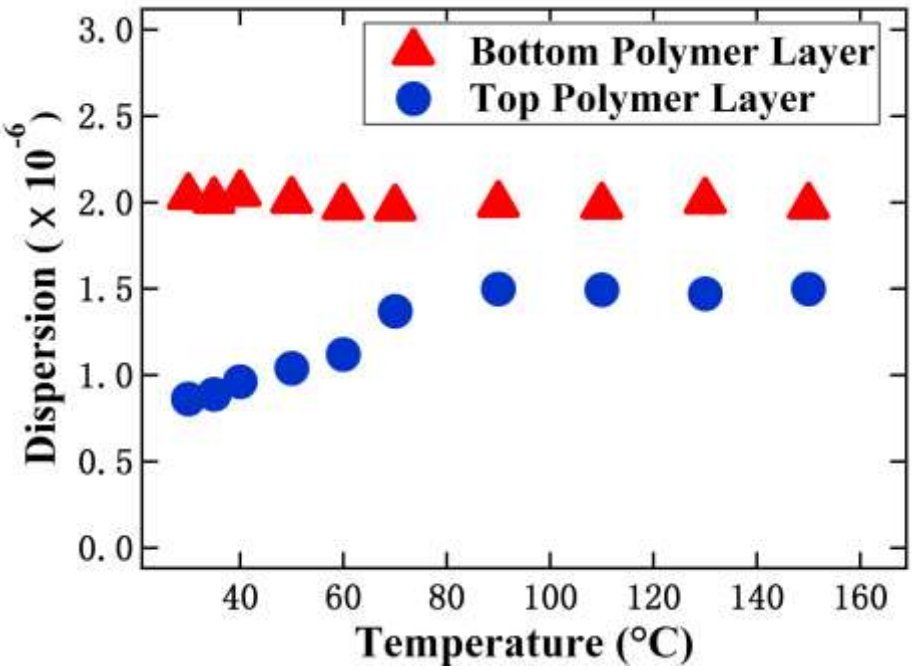

Figure 3-13 Plot of the density of the adsorbed layer as a function of annealing time

In this experment, we can also obtain the disperson value of the PEO adsorbed layer based on the x-ray reflectiviy data. As shown in Figure 3-13, the bottom high density layer ($\delta=2.0 \times 10^{-6}$) doesn't change with increasing temperature. However, the top layer shows an increase from in δ value from 0.8×10^{-6} to 1.6×10^{-6} with the elevating temperautre. Note that the film was annealed for 5 h before XR measurement so that the original δ value is slightly lower than the bulk value($\delta_{PEO}=1.26 \times 10^{-6}$).

Conclusions

We have investigated the annealing time dependence of the poly (ethylene oxide) (M_w=20k) adsorbed layer thickness by using ellipsometry, atomic force microscopy (AFM) and x-ray reflectivity techniques. We found that the thickness of the adsorbed layer is about 30 Å regardless of the original film thickness.

We also found that the PEO adsorbed layer consists of two layers, that is the top bulk-like density layer and the bottom high density layer. The total thickness of the PEO adsorbed layer remains almost constant with increasing the annealing time. This is different from that of PS adsorbed layer previously reported.

The formation of the irreversibly adsorbed layer can be divided into two stages. The early stage is single chain adsorption and surface saturation. The attachment of arriving monomers is virtually instantaneous on reaching the surface. After attachment of the first monomers, the collapse of a single chain into a flattened structure occurs. It is important to add that in dilute polymer solutions, chains collapse into flattened configurations without hindrance from others. The later stage is the formation of the tenuously attached outer loops, since free surface sites for late-coming chains become scarce. The observation of the AFM images didn't show obvious crystalline structure in the PEO adsorbed layer. By analysis with the diffuse limited aggregation (DLA) model, maybe it is difficult for the adsorbed layer to form crystal structures.

Further $scCO_2$ leaching experiments proved that the adsorbed layer prepared by the toluene leaching is the final structure. This is consistent with the PS adsorbed layer composed of low M_w. we postulate that the chain length is too short to form the loops between the empty sites.

The temperature dependence of the PEO adsorbed layer thickness were investigated by using x-ray reflectivity. We found that the contraction and expansion of the PEO adsorbed layer is thermally reversible. The top layer becomes more denser with increasing T, while the bottom layer doesn't change the density.

Although there is a growing literature on the crystallization of polymer in ultrathin films, we still lacking a clear understanding of the adsorption and crystallization of in thin and ultrathin films, especially close to the interfaces. We need to clarify how such an adsorbed layer influence the structural properties of polymer thin films.

References

[1] A.G. Emslie, F.T. Bonner, L.G. Peck, Journal of Applied Physics, 29 (1958) 858-862.

[2] C.J. Lawrence, Physics of Fluids, 31 (1988) 2786-2795.

[3] D. Meyerhofer, Journal of Applied Physics, 49 (1978) 3993-3997.

[4] C.W. Frank, V. Rao, M.M. Despotopoulou, R.F.W. Pease, W.D. Hinsberg, R.D. Miller, J.F. Rabolt, Science, 273 (1996) 912-915.

[5] D.E. Bornside, Macosko, C.W., Scriven, L.E., Journal of imaging technology, 13 (1987) 122-130.

[6] M.K. Mundra, C.J. Ellison, R.E. Behling, J.M. Torkelson, Polymer, 47 (2006) 7747-7759.

[7] A. Brûlet, F. Boué, A. Menelle, J.P. Cotton, Macromolecules, 33 (2000) 997-1001.

[8] J.G.-T.a.B. Jérôme, Colloid & Polymer Science, 285 (2007) 1617-1623.

[9] J. Perlich, V. Körstgens, E. Metwalli, L. Schulz, R. Georgii, P. Müller-Buschbaum, Macromolecules, 42 (2008) 337-344.

[10] G. Reiter, P.G. de Gennes, The European Physical Journal E: Soft Matter and Biological Physics, 6 (2001) 25-28.

[11] W.J. Orts, J.H. van Zanten, W.-l. Wu, S.K. Satija, Physical Review Letters, 71 (1993) 867-870.

[12] G. Reiter, M. Hamieh, P. Damman, S. Sclavons, S. Gabriele, T. Vilmin, E. Raphael, Nat Mater, 4 (2005) 754-758.

[13] G. Reiter, S. Napolitano, Journal of Polymer Science Part B: Polymer Physics, 48 (2010) 2544-2547.

[14] Y. Fujii, Z. Yang, J. Leach, H. Atarashi, K. Tanaka, O.K.C. Tsui, Macromolecules, 42 (2009) 7418-7422.

[15] S. Peter, H. Meyer, J. Baschnagel, Journal of Polymer Science Part B: Polymer Physics, 44 (2006) 2951-2967.

[16] J.H. Kim, J. Jang, W.-C. Zin, Langmuir, 16 (2000) 4064-4067.

[17] D.S. Fryer, P.F. Nealey, J.J. de Pablo, Macromolecules, 33 (2000) 6439-6447.

[18] J.L. Keddie, R.A.L. Jones, R.A. Cory, EPL (Europhysics Letters), 27 (1994) 59.

[19] J.L. Keddie, R.A.L. Jones, R.A. Cory, Faraday Discussions, 98 (1994) 219-230.

[20] H.K. Nguyen, D. Prevosto, M. Labardi, S. Capaccioli, M. Lucchesi, P. Rolla, Macromolecules, 44 (2011) 6588-6593.

[21] K. Dalnoki-Veress, J.A. Forrest, M.V. Massa, A. Pratt, A. Williams, Journal of Polymer Science Part B: Polymer Physics, 39 (2001) 2615-2621.
[22] J.-U. Sommer, G. Reiter, The Journal of Chemical Physics, 112 (2000) 4384-4393.
[23] Y. Samoshina, T. Nylander, V. Shubin, R. Bauer, K. Eskilsson, Langmuir, 21 (2005) 5872-5881.
[24] M. Aubouy, O. Guiselin, E. Raphaël, Macromolecules, 29 (1996) 7261-7268.
[25] P. Auroy, L. Auvray, L. Leger, Macromolecules, 24 (1991) 2523-2528.
[26] B. O'Shaughnessy, D. Vavylonis, Physical Review Letters, 90 (2003) 056103.
[27] T. Miyazaki, K. Nishida, T. Kanaya, Physical Review E, 69 (2004) 061803.
[28] T. Koga, J. Jerome, M.H. Rafailovich, B. Chu, J. Douglas, S. Satija, Advances in Colloid and Interface Science, 128–130 (2006) 217-226.
[29] Y. Yang, M.M.-C. Cheng, X. Hu, D. Liu, R.J. Goyette, L.J. Lee, M. Ferrari, Macromolecules, 40 (2007) 1108-1111.
[30] Q. Lan, J. Yu, J. Zhang, J. He, Macromolecules, 44 (2011) 5743-5749.
[31] M.F. Kemmere, Supercritical Carbon Dioxide for Sustainable Polymer Processes, in: Supercritical Carbon Dioxide, Wiley-VCH Verlag GmbH & Co. KGaA, 2006, pp. 1-14.
[32] F.-H. Huang, M.-H. Li, L. Lee Lloyd, E. Starling Kenneth, H. Chung Frank T, Journal of Chemical Engineering of Japan, 18 (1985) 490-496.
[33] X. Wang, I.C. Sanchez, Langmuir, 22 (2006) 9251-9253.
[34] T. Koga, Y.S. Seo, X. Hu, K. Shin, Y. Zhang, M.H. Rafailovich, J.C. Sokolov, B. Chu, S.K. Satija, EPL (Europhysics Letters), 60 (2002) 559.
[35] K. Devanand, J.C. Selser, Macromolecules, 24 (1991) 5943-5947.
[36] E.C. Cooper, P. Johnson, A.M. Donald, Polymer, 32 (1991) 2815-2822.